Design of an LMI-based Linear Quadratic Pole Placement Controller for Quadcopters

A. G. Ibrahim[1*], J. D. Jiya[2], E. C. Anene[2]

[1]Department of Mechatronics and Systems Engineering, Abubakar Tafawa Balewa University, Bauchi, Bauchi State, Nigeria
[2] Department of Electrical and Electronics Engineering, Abubakar Tafawa Balewa University, Bauchi, Bauchi State, Nigeria

ABSTRACT: Quadcopter systems have become part of the aviation industry with their applications seen in surveillance, search and rescue, photography and so on. Proportional-Integral-Derivative (PID) and Linear Quadratic Regulator (LQR) control techniques do not provide robust performance of quadcopters due to their extensive tuning requirements, and the non-linear and coupled nature of the system dynamics. This paper presents an approach which combines Linear Quadratic Regulator (LQR) and Pole-Placement (PP), coined Linear Quadratic Pole Placement (LQPP) to design the state feedback gain matrix for the attitude and position control of the quadcopter system. The pole placement region was selected as the intersection between a strip region, and a disk region within the stability region for the poles. The optimization problem was to minimize the cost function of the Algebraic Riccati equation, which penalizes the control effort, and the system states. The pole locations are then used as constraints and then cast as linear matrix inequalities (LMI). The mathematical model for the dynamics and kinematics of the quadcopter system is presented, and the LMI-based design concept for the LQPP is also formulated. The dominant poles of the quadcopter system are utilized for pole placement, while the remaining poles are used to minimize the cost function of the linear quadratic regulator. Simulation results using MATLAB/Simulink 2019b demonstrate that the optimized controller significantly reduces overshoot by 5.66% and 7.24% for the position and attitude responses respectively and settling time by 9.05% and 7.93% for the position and attitude responses respectively compared to the unoptimized LQPP controller. The results demonstrate that the LQPP design markedly improves attitude and position control, offering a robust and efficient solution for quadcopter stabilization. This approach paves the way for deployment in precision-critical missions such as infrastructure inspection, search and rescue, and dynamic aerial mapping.

KEYWORDS: Quadcopter, LMI, Pole-placement, Attitude Control, Optimization.

[Received Dec. 27, 2024; Revised May 24, 2025; Accepted Aug, 13, 2025] Print ISSN: 0189-9546 | Online ISSN: 2437-2110

I. INTRODUCTION

Unmanned Aerial Vehicles (UAVs), also called Remote Piloted Vehicles (RPVs) or drones, are vertical take-off and landing (VTOL) aerial vehicles, that have become part of the aviation world in the past few decades largely due to advances in micro-electromechanical systems (MEMS) technology and advanced control design and implementation techniques. UAVs are receiving a lot of attention now due to their applications in our everyday lives (Mardijah, 2022). The applications of these UAVs can be found in military operations, ranging from reconnaissance missions to deployment of missiles, in agriculture for spraying of pesticides and insecticides, mapping and pest control, in photography and disaster management for areas not easily accessible on land, border surveillance and control, search and rescue missions, law enforcement, pipeline inspection and monitoring and parcel delivery (Ahmadi Dastgerdi *et al*., 2022; Amiruddin *et al*., 2021; Aslam & Bilal, *2024*; Morbale *et al*., 2022; Karam *et al.,* 2024). Developments in UAV technology have also opened a lot of opportunities in research and development in the fields of control design and testing, modelling and simulations, structural design and fabrication, sale and services (Pounds *et al*., 2010; Howard & Merz, 2015; Andersson *et al.*, 2017; Carrio *et al.*, 2017). The quadcopter (or quadrotor) is a UAV with four fixed-pitched rotors, and has six degrees of freedom, making it an under-actuated system. It also exhibits open loop instability, making its control a challenging task. There are two basic configurations of the quadcopter: the '+' configuration, and the 'x' configuration. The 'x' configuration is considered to be more stable in terms of operations (Thu and Gavrilov, 2017). Due to its under-actuation, the control of the quadcopter becomes increasingly difficult in the event of a failure of any of the actuators.

Classical controller like PID and LQR methods are not robust to non-linearity and coupled nature of the system dynamics of the quadcopter (Sahrir & Mohd Basri, 2022). Much research has focused on the development of control algorithms for the attitude and altitude control of quadcopter systems. Ahmad *et al.* (2020) developed an LQR controller for the position and yaw control of a quadcopter system, the results indicate that the steady error in the altitude can be reduced by applying an integrator in the feedback loop of the controller.

*Corresponding author: agibrahim@atbu.edu.ng

doi: http://dx.doi.org/10.63746/njtd.v22i4.3215

Similarly, Xu *et al* (2016) designed an LQR plus integrator stabilization of a quadcopter system, and compared the results with those of an L1 adaptive controller. Okyere *et al.* (2019) designed an LQR controller for a quadcopter system. The tuning of the controller focused on the design of the feedback gain matrix, and the performance specifications of the controller were analysed. Tengis & Batmunkh (2017) designed a full-state feedback controller for quadcopter systems by pole placement technique. The results show that the quadcopter can track the attitude references with minimal errors. Reizenstein (2017) carried out a comparative analysis of the performance of LQR and PID-controlled quadcopter systems. The results indicated that the LQR-controlled system gave a better performance compared to the PID-controlled system. Yoon & Doh (2022) explored the stabilization of quadcopters using optimal PID gains determined through machine learning rather than expert inputs. A long short-term memory (LSTM) neural network was trained, however the accuracy is influenced by the quality and diversity of the training data used. Cedro *et al*., (2024) designed an adaptive PID control system for quadcopters, where controller parameters are adjusted based on real-time mass identification using the weighted recursive least squares (WRLS) method. Experimental validation using a National Instruments myRIO-1900 controller demonstrated improved stability, reduced measurement noise, and optimized PID tuning through the Gauss–Newton method.

This paper developed a linear matrix inequality (LMI)-based optimized linear quadratic pole placement (LQPP) controller for attitude and position control of a quadcopter system with a view to increase performance and robustness. The constraints from the Riccati equation of the linear quadratic regulator (LQR) and pole placement (PP) are cast together as LMIs, and the state feedback gain matrix is determined. The stability region for the pole placement is the intersection of disk and strip regions.

The rest of the paper is organized as follows: the kinematic and dynamic equations governing the operations of the quadcopter are presented in section II, the problem formulation and methodology adopted are presented in section III, the results obtained, and the analysis carried out are presented in section IV, and finally, conclusions are drawn in section V.

II. KINEMATIC AND DYNAMIC MODEL OF QUADCOPTER

Consider the quadcopter system presented in Figure 1, the inertial frame is defined by ϕ, θ, ψ , while the earth frame is defined by X,Y,Z. the four motor are defined as M_1 through M_4, while the thrusts generated by the motors are defined as T_1 through T_4 and *m* is the mass of the quadcopter.

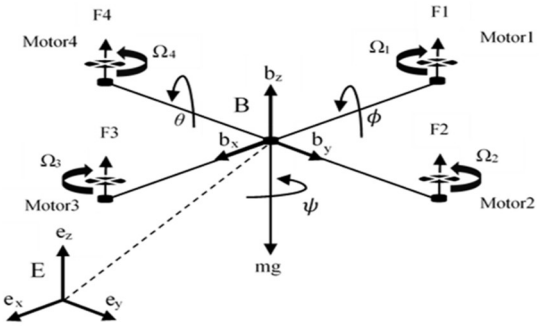

Figure 1 General architecture of quadcopters with 'x' configuration

The dynamic model equations of the quadcopter are described by the translational motion dynamics and the rotational motion dynamics. The translational and rotational motions of the quadcopter are described in equations (1) – (6) (Nguyen & Hong, 2019).

$$\ddot{x} = (U_z(\cos\varphi\sin\theta\cos\psi + \sin\varphi\sin\psi) - K_x\dot{x})/m \quad (1)$$

$$\ddot{y} = (U_z(\cos\varphi\sin\theta\sin\psi - \sin\varphi\sin\psi) - K_y\dot{y})/m \quad (2)$$

$$\ddot{z} = -g + (U_z(\cos\varphi\cos\theta) - K_z\dot{z})/m \quad (3)$$

$$\ddot{\varphi} = (U_\varphi + (I_{yy} - I_{zz})\dot{\theta}\dot{\psi} - J_T\dot{\theta}\Omega - K_\varphi\dot{\varphi})/I_{xx} \quad (4)$$

$$\ddot{\theta} = (U_\theta + (I_{zz} - I_{xx})\dot{\varphi}\dot{\psi} - J_T\dot{\varphi}\Omega - K_\theta\dot{\theta})/I_{yy} \quad (5)$$

$$\ddot{\psi} = (U_\psi + (I_{xx} - I_{yy})\dot{\varphi}\dot{\theta} - K_\psi\dot{\psi})/I_{zz} \quad (6)$$

Where $\ddot{x}, \ddot{y}, \ddot{z}$ represent the linear acceleration along the *x*, *y* and *z* axes, $\dot{x}, \dot{y}, \dot{z}$ represent the liner velocity of the quadcopter, I_{xx}, I_{yy}, I_{zz} represent the moments of inertia along the x, y, z directions, $K_\varphi, K_\theta, K_\psi, K_x, K_y, K_z$ represent the drag coefficients for the roll, pitch, yaw, and the *x*, *y*, *z* positions respectively, which depend on the flight conditions. J_T is the moment of inertia of each motor, while Ω represents the angular velocity of the motors. m is the total mass of the quadcopter system, φ, θ, ψ are the roll, pitch and yaw angles respectively, and $\dot{\phi}, \dot{\theta}, \dot{\psi}$ represent the roll, pitch and yaw rates respectively. $U_\varphi, U_\theta, U_\psi$ are the torques in the roll, pitch and yaw Euler angles respectively. The four control inputs of the quadcopter according to Nguyen & Hong (2019) are presented in equation (7).

$$\begin{aligned} U_z &= F_1 + F_2 + F_3 + F_4 \\ U_\varphi &= (F_4 - F_2)L \\ U_\theta &= (F_3 - F_1)L \\ U_\psi &= \tau_1 - \tau_2 + \tau_3 - \tau_4 \end{aligned} \quad (7)$$

where $\tau_i = d\Omega_i^2$ and $F_i = b\Omega_i^2$ are the torque and thrust forces produced by the *i*-th motor, *b* and *d* are positive constants (thrust and drag coefficients respectively). These coefficient s depend on physical parameters such as air density, propeller radius, blade count and propeller geometry. Ω_i is the angular

velocity of the *i*-th motor, and U_z is the total thrust generated by the motors, $U_\varphi, U_\theta, U_\psi$ are the torques in the roll, pitch and yaw Euler angles respectively. *L* is the length of the arm of the quadcopter from the centre.

Table 1 presents the values of the components of the quadcopter. The quadcopter F450 developed by Da-jiang Innovations (DJI) was considered for this work.

Table 1 List of values of the quadcopter F450 parameters (Nguyen and Hong, 2018)

Parameter	Description	Value
m	Mass	$2kg$
L	Arm length	$0.225m$
b	Thrust Coefficient	$9.8\times10^{-6}\ N/m^2$
$\mathbf{I_{xx}, I_{yy}, I_{zz}}$	Moment of Inertia	0.0035, 0.0035, $0.005kg/m^2$
g	Acceleration due to gravity	$9.8m/s^2$
$\mathbf{J_T}$	Rotor Inertia	$2.8\times10^{-6}\ kg.m^2$

III. METHODOLOGY

A. PROBLEM FORMULATION

The linear quadratic pole placement (LQPP) controller is an optimal combination of linear quadratic regulator (LQR) and pole placement controller designed to improve robustness. For the LQR quadratic performance index given in equation (8) (Babawuro *et al* 2020; Deng *et al* 2017), the control objective is to utilize LMI techniques to find the state feedback gain matrix *K* of the LQPP controller, which combines the energy minimization property of the linear quadratic regulator with the performance of the pole placement technique. The LQPP technique utilizes the dominant eigenvalues of the system by placing them within a specified region, while the remaining eigenvalues of the system are used to minimize the quadratic performance index (Ka, 2002)

$$J = \int_0^\infty \left[x^T(t) Q x(t) + u^T R u(t) \right] dt \tag{8}$$

Where *J* is the cost function to be minimized, Q is the $m \times m$ dimensional symmetric non-negative matrix, which is the weighting matrix of the state variables x in the performance index, while R is the $n \times n$ dimensional symmetric matrix, which is the weighting matrix of the control input signals *u(t)*.

This implies that the closed loop eigenvalues λ_{ni} of the system responsible for the performance are selected for placement in the specified region, while the remaining poles are used for energy minimization using the quadratic cost function. This is presented in equation (9) (Ka, 2002).

$$\lambda(A - BK) = \left\{ \underbrace{(\lambda_1, \ldots \lambda_{n1})}_{PP}, \underbrace{(\lambda_{n1+1}, \ldots \lambda_n)}_{LQ} \right\} \tag{9}$$

Where λ the eigenvalues of the system, A, B are are the system matrix, and input matrix respectively, and *K* is the feedback gain matrix.

The computation of the feedback gain matrix is performed using equation (10)

$$K = R^{-1} B^T P \tag{10}$$

Where the matrix *P* is a positive definite matrix obtained from the solution of the algebraic Riccati equation given in equation (11) (Martins *et al.,* 2019), with *Q* being a symmetric non-negative matrix.

$$A^T P + PA - PBR^{-1}P + Q = 0 \tag{11}$$

Where *A* is the system matrix, *P* is a positive definite matrix, *B* is the output matrix, and *Q* and *R* are weighting matrices which penalize the system state and control input respectively.

B. LMI-BASED OPTIMIZATION OF LQPP

The algebraic Riccati equation can be expressed as LMIs given in inequalities (12) – (15).

$$\begin{bmatrix} A^T P + PA + Q & PB \\ B^T P & -R \end{bmatrix} < 0 \tag{12}$$

$$P = P^T > 0 \tag{13}$$

$$Q > 0 \tag{14}$$

$$R > 0 \tag{15}$$

Figure 2 shows the block diagram of the quadcopter model with the state feedback gain matrix, which is optimized using LMI. Consider the state equation of the quadcopter presented in equation(16).

$$\begin{aligned} \dot{x} &= Ax + Bu \\ y &= Cx + Du \end{aligned} \tag{16}$$

Where *A, B, C, D* are the system matrix, input matrix, output matrix, and transmission matrix of the system respectively.

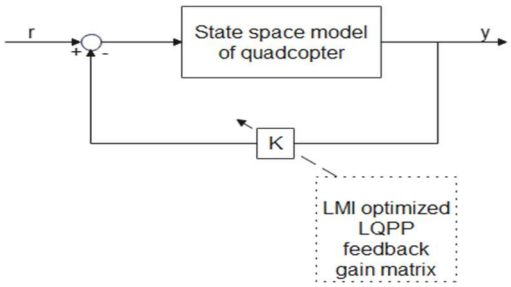

Figure 2 Block diagram of state feedback LQPP regulator

The control signal is fed through the feedback gain matrix, and can be expressed as;

$$u = r - Kx \tag{17}$$

Where r is the vector of reference inputs, x are the states of the quadcopter system, and *K* is the feedback gain matrix, which is to be optimized using LMI technique. For the regulator problem, the reference input is zero, hence, $u = -Kx$

substituting the value of *u* into equation(16), gives

$$\dot{x} = Ax + B(-Kx) \tag{18}$$

$$\dot{x} = (A - BK)x \tag{19}$$

$$\dot{x} = A_m x \tag{20}$$

$$A_m = A - BK \tag{21}$$

Where A_m is the closed loop system matrix, which is Hurwitz.

The system described by equation (21) is asymptotically stable if all the poles lie in the left-hand plane of an argand diagram. However, system stability alone does not lead to satisfactory system performance, hence the position of the poles in the left-hand plane have to be forced to lie within the LMI region given in Figure 3. For the proposed stabilizing controller, a combination of the strip region $\left(\mathrm{H}_{a,b}\right)$ and the disk region $\left(D_{c,r}\right)$ as shown in Figure 3. The strip region is indicated by the dash-shaded region, while the disk region is indicated by the dot-shaded region. The radius of the disk is given by *r*, and *c* is the center of the disk. In the strip region $\left(\mathrm{H}_{a,b}\right)$, the stability region requires that all the eigenvalues of the matrix *A* of the system are located in the strip region.

$$\mathrm{H}_{a,b} = \left\{x + jy \mid -b < x < -a\right\} \tag{22}$$

Where $x + jy$ is the pole location, and *-b, -a* are the maximum and minimum values of the boundary respectively. This can be described by the equation (22). The system matrix $A \in \square^{n\times n}$ given in equation (16) is $\mathrm{H}_{a,b}$ -stable if and only if there exists a matrix $P \in S^n$ which satisfies the following LMI conditions presented in inequalities (23) – (27).

$$P > 0 \tag{23}$$

$$A_m^T P + PA_m + 2aP < 0 \tag{24}$$

$$A_m^T P + P_m A + 2bP > 0 \tag{25}$$

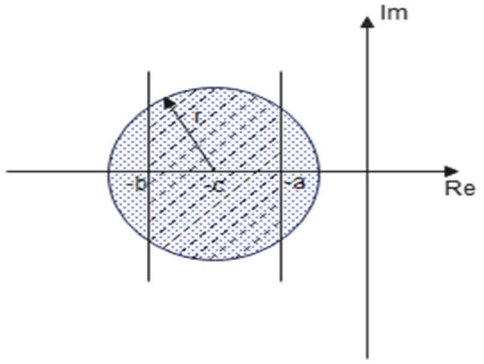

Figure 3 LMI region for the pole placement, consisting of the intersection of the disk and strip regions.

Furthermore, the constraints of the pole placement state feedback controller in the LMI region of the controller are presented in LMI form in (26) – (31) as presented in Duan & Yu (2013).

Substituting the value of equation (21) into inequalities (24) and (25), and simplifying, yields inequalities (26) and (27) .

$$AP + PA^T + BM + M^T B^T + 2aP < 0 \tag{26}$$

$$AP + PA^T + BM + M^T B^T + 2bP > 0 \tag{27}$$

Where $M = KP$

In the disk region $\left(D_{c,r}\right)$, the stability region requires that all the eigenvalues of the matrix *A* of the system are located in the disk region described by equation (28).

$$D = D_{(c,r)} = \left\{x + jy \mid \left(x + c\right)^2 + y^2 < r^2\right\} \tag{28}$$

Where *c, r* represent the centroid of the disk, and disk radius respectively.

The system is $D_{(c,r)}$ -stable if and only if there exists a matrix $P \in S^n$ which satisfies the LMI conditions presented in inequalities (29) and (30).

$$P > 0 \tag{29}$$

$$\begin{bmatrix} -rP & cP + A_m P \\ cP + PA^T & -rP \end{bmatrix} < 0 \tag{30}$$

Substituting equation (21) into inequality(30), and simplifying yields the LMI presented in inequality (31).

$$\begin{bmatrix} -rP & cP + PA^T + M^T B^T \\ cP + AP + BM & -rP \end{bmatrix} < 0 \tag{31}$$

Hence, the intersection between the strip and disk region constraints must be satisfied in order to meet the performance specifications. This can be expressed as presented in equation (32).

$$D = \mathrm{H}_{(a,b)} \bigcap D_{(c,r)} \tag{32}$$

The inner loop stabilizing controller for the quadcopter system is hence formulated from a combination of LQR and pole placement techniques to design a robust controller while maintaining performance requirements. The LMI-based optimization minimizes the quadratic cost function expressed in equation (8) subject to the constraints represented by the LMIs, which ensure that the system performance response is improved. Furthermore, the controller gain is iteratively adjusted using the LMI-based algorithm to find the best solution that optimizes the performance while adhering to the stability constraints.

IV. RESULTS AND DISCUSSION

A. POSITION RESPONSE OF OPTIMIZED LQPP FOR QUADCOPTER CONTROL

The linear matrix inequality (LMI)-based optimized linear quadratic pole placement controller (LQPP), which was designed as a baseline controller for the quadcopter system was tested in simulation using MATLAB 2019b. The resulting inner loop controller gain matrix from the nominal design using LQR and the LMI-optimized design using LQPP are presented in equations (33) and (34) respectively.

$$K_1 = \begin{bmatrix} -11.46 & -5.05e\text{-}14 & -8.86 & -1.57e\text{-}14 & 14.90 & 6.26 & -7.07 & -4.15e\text{-}14 & -4.99 & -1.32e\text{-}13 & 56.49 & 5.00 \\ -3.31e\text{-}15 & -11.46 & -8.86 & -14.90 & -1.17e\text{-}14 & -6.26 & -3.85e\text{-}14 & -7.07 & -4.99 & -56.49 & -3.75e\text{-}14 & -4.99 \\ 11.46 & -3.48e\text{-}14 & -8.86 & -3.27e\text{-}14 & -14.90 & 6.26 & 7.07 & -2.91e\text{-}14 & -4.99 & -1.92e\text{-}13 & -56.49 & 4.99 \\ -1.15e\text{-}14 & 11.46 & -8.86 & 14.90 & 9.07e\text{-}15 & -6.26 & 1.18e\text{-}14 & 7.07 & -5.00 & 56.49 & 7.88e\text{-}14 & -5.00 \end{bmatrix} \quad (33)$$

$$K_{1(qpt)} = \begin{bmatrix} -2.22e\text{-}14 & -4.28e\text{-}14 & -15.77 & -8.61e\text{-}16 & 5.38e\text{-}15 & -1.29e\text{-}15 & -1.65e\text{-}14 & -7.38e\text{-}14 & -31.62 & -2.25e\text{-}14 & 2.13e\text{-}13 & -5.49e\text{-}14 \\ 1.11e\text{-}14 & 15.27 & -1.62e\text{-}14 & 11.04 & 9.51e\text{-}16 & 1.64e\text{-}15 & 8.37e\text{-}15 & 10.00 & 2.91e\text{-}15 & 65.39 & 3.58e\text{-}15 & 1.40e\text{-}13 \\ -15.27 & 4.67e\text{-}14 & -1.95e\text{-}14 & -6.37e\text{-}15 & 11.04 & -6.12e\text{-}17 & -9.99 & 6.26e\text{-}14 & -5.81e\text{-}14 & 1.98e\text{-}13 & 65.39 & -3.89e\text{-}15 \\ 2.15e\text{-}14 & 3.17e\text{-}14 & -5.26e\text{-}15 & -1.31e\text{-}16 & -9.50e\text{-}16 & 10.90 & 2.82e\text{-}14 & 6.87e\text{-}14 & -2.32e\text{-}14 & 4.013e\text{-}14 & -4.78e\text{-}14 & 31.62 \end{bmatrix} \quad (34)$$

The response to a unit step input for the *x*, *y* and *z* positions are presented in

Figure 4 - 6. The position response of the LMI-optimized LQPP compared with the nominal LQPP designed for the quadcopter system shows a decrease in the rise time, settling time and overshoot when the LMI-LQPP is deployed. From Table 2, it is shown that the rise time and the settling time are reduced by 0.22% and 2.64% respectively of the quadcopter system. There is also a reduction of 2.76% in the overshoot of the response.

In this study, a linear quadratic pole placement (LQPP) controller was designed to ensure the stability of the quadcopter system. This controller combines the principles of linear quadratic regulation (LQR), which minimizes a cost function balancing state deviation and control effort, with pole placement techniques to position the closed-loop system poles at specific locations for desired performance characteristics. To optimize the controller parameters, Linear Matrix Inequality (LMI) techniques were employed, transforming the design problem into a convex optimization framework that ensures stability and performance (De Oliveira & Zheng, 2022). The effectiveness of this optimized controller was assessed by comparing its attitude and position responses against those of the nominal LQPP, providing insights into the improvements achieved through this approach.

The feedback gain values of the nominal controller presented in equation (33) contain larger values compared to the optimized values presented in equation (34), which implies that the controlled quadcopter system will have improved performance, improved stability and reduced overshoot (Fatkhullin and Polyak, 2020). Furthermore, the reduced parameter values of the feedback gain matrix imply that the control effort is reduced because the objective function penalises the control effort, thereby reducing the energy dissipated (Lin *et al.*, 2022; Wilt & Sands, 2022). This indicates a more efficient and effective control strategy, due to better utilization of the system's dynamics and the enhanced design objectives through LMI-based optimization. For the quadcopter system, this translates to smoother operation, improved energy efficiency, and increased component longevity.

The position control responses for the *x* and *y* positions presented in Figures 4 -5 show that the optimized controller exhibited a 0.22% increase in rise time and 2.64% increase in settling time for the both the *x* and *y* position responses compared to the nominal controller. From table 2, the results also showed a 2.76% reduction in overshoot in both cases, and faster convergence to the desired position by 0.054s, compared to the nominal response. Formulating the LQPP controller as an LMI optimization problem allows for the constraints on closed-loop pole locations to be placed within the specified intersection between the disk and strip region, which ensures that the desired transient response in terms of oscillating frequency and damping is achieved. This ensures improved settling time, reduced overshoot, and precise rise time bounds while maintaining convexity. Similarly, the altitude (*z*) response presented in Figure 6 also showed that the rise and settling times response of the LMI-optimized controller decreased by 7.09%, and 2.14% respectively. Although, the overshoot increased insignificantly by 0.2%, this is expected due to the reduction in the rise time and settling times (Gonzalez-Villagomez *et al.*, 2023). The convex nature of LMIs yields globally optimal solutions that automatically balance transient performance and stability, thus, eliminating manual trial-and-error.

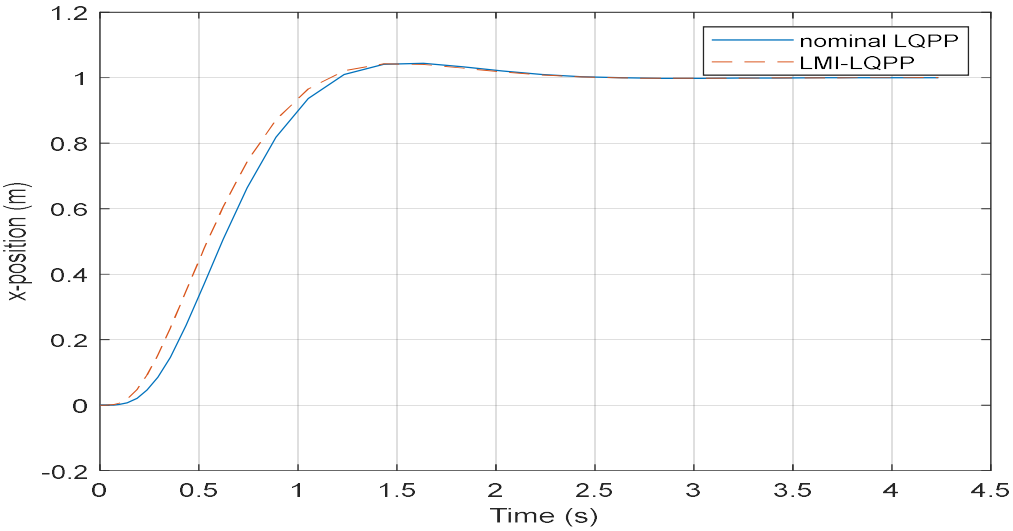

Figure 4 Unit step response in X-position for nominal and LMI optimized LQPP

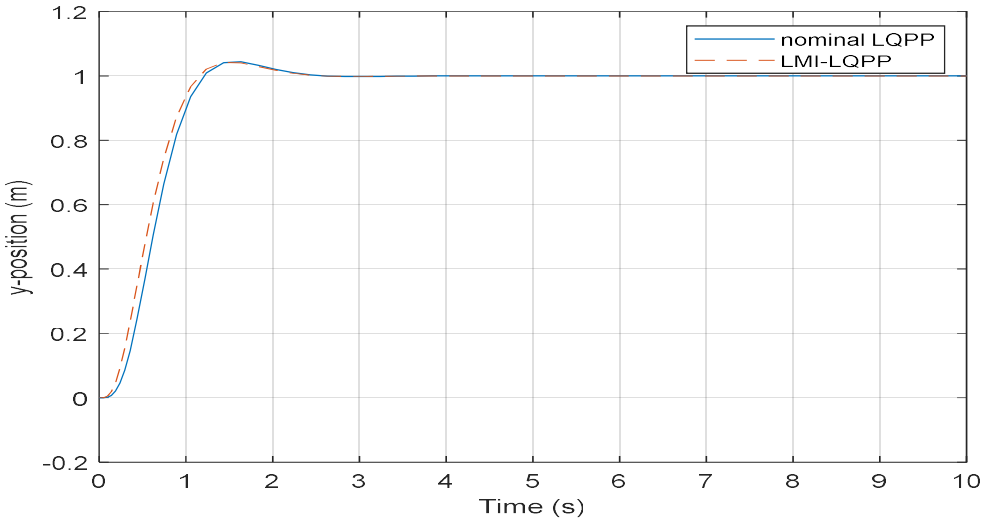

Figure 5 Unit step response in Y-position for nominal and LMI Optimized LQPP

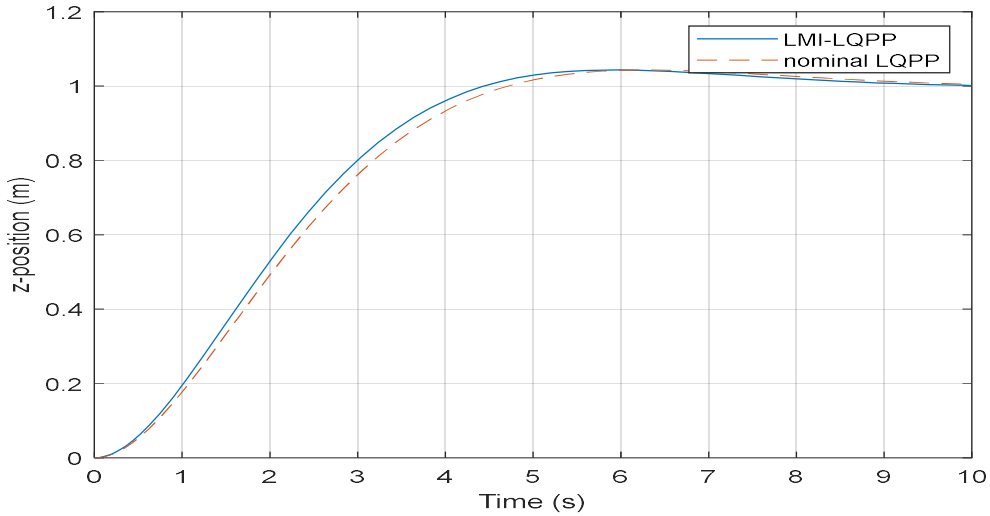

Figure 6 Unit Step Response in Altitude (z) for LQPP and LMI-LQPP

Table 2 Comparison of the performance of nominal LQPP and LMI-LQPP for position

Position		Rise time (s)	Settling time (s)	Overshoot (%)	Undershoot (%)	Peak	Peak time (s)
x	Nominal LQPP	0.6945	2.0442	4.35	5.99×10^{-74}	1.044	1.643
	LMI-LQPP	0.6930	1.9902	4.23	3.44×10^{-73}	1.042	1.434
y	Nominal LQPP	0.6945	2.0442	4.35	5.99×10^{-74}	1.044	1.643
	LMI-LQPP	0.6930	1.9902	4.23	3.44×10^{-73}	1.042	1.434
z	Nominal LQPP	2.4679	8.0866	4.31	0	1.0431	6.3778
	LMI-LQPP	2.2930	7.9135	4.32	0	1.0432	5.9868

B. ATTITUDE RESPONSE OF OPTIMIZED LQPP FOR QUADCOPTER CONTROL

The response of the roll, pitch and yaw of the quadcopter system to a unit step input is presented in Figure 7 - 9 and indicated a reduction in the overshoot and undershoot of the LMI-LQPP compared to the nominal LQPP responses. Similarly, the rise time is reduced, but the settling time appears the same. From Table 3, it can be inferred that there is a 36% decrease in the rise time, and an 84.57% decrease in the overshoot. Although, the results also indicated a 1.31% increase in the undershoot when the LMI-LQPP is deployed, the settling time did not change significantly since only a 2.5% increase is recorded for the LMI-LQPP. The performance to step response of the pitch angle indicated a 0.82% reduction in the rise time, and a 5.56% reduction in settling time. The percentage overshoot was reduced by 35.96% when the LMI-LQPP was deployed compared to the nominal LQPP, although, the undershoot was increased by 8.23%. The performance of the LMI-optimized LQPP feedback controller for the yaw response indicate that there is a 24.3% decrease in the rise time in the yaw response to a step input when the LMI-LQPP is applied compared to the nominally designed LQPP. Similarly, the overshoot in the response is increased by 8.36%, although, the undershoot is reduced by 32.95%. the settling time increased by just 0.01%. Overall, the settling time decreased by 7.24% and 7.93% respectively for the position and attitude responses, while the overshoot decreased by 5.66% and 9.05% respectively for the position and attitude responses when the LMI-optimized LQPP controller was deployed for the quadcopter system against the nominally designed LQPP.

The attitude responses revealed that the optimized LQPP controller significantly outperformed the nominal controller in stabilizing the quadcopter's attitudes. From 3, the rise time was reduced by 36% and the overshoot by 85%. However, the response exhibits undershoot, which is caused by the non-minimum phase nature of the roll model (Bose *et al.*, 2019; Li & Shieh, 2000). Similarly, from **Error! Reference source not found.**3, it is shown that the pitch response rise and settling times reduced by 0.83% and 5.56% respectively, while the overshoot reduced by 35.96%, although there is an increase of 8.23% in the undershoot. In an attempt to reduce the transient response of the pitch, the controller increased the undershoot. This was caused due to the unconstrained non-minimum phase behaviour of the system. The response to a unit step for the yaw control of the quadcopter system was presented in Figure 9 for both the nominal and optimized LQPP. The transient response presented in 3 show that the rise time increased by 24.3% for the optimized controller response, while the overshoot also increased by 8.36%, however, the undershoot was decreased by 32.95%, and a 0.01% increase in the settling time. The yaw control proved challenging to improve because the net yaw torque depends on the drag differential between clockwise and counterclockwise rotors, which severely limits the control effort, and usually forces the motors near saturation. Furthermore, aggressive roll and pitch maneuverers introduce gyroscopic and aerodynamic coupling that causes unintended yaw precession. Finally, commanding large yaw rates can saturate actuators and

starve the roll and pitch loops of authority, leading to oscillations and degraded performance.

These improvements stem from the LMI optimization, which enables precise pole placement to shape the system's transient response, enhancing damping and reducing oscillations (Rezende *et al.*, 2021). Furthermore, the steady-state error was reduced exponentially to zero, as the attitude responses were able to track the reference signal, this ensure that the system exhibits bounded-input-bounded-output (BIBO) stability. The results demonstrate greater accuracy in maintaining the desired orientation and enhanced performance, which is critical for quadcopter applications requiring stable hovering or precise attitude control, such as aerial surveillance or data collection.

Overall, the integration of LMI techniques with LQPP offers substantial benefits for quadcopter stability and control. The optimized controller not only improves key metrics like settling time, overshoot, and steady-state error but also enhances stability, making it well-suited as a stabilizing controller for quadcopters. Nonetheless, the formulation of the non-minimum phase behaviour as an LMI constraint limits the performance of the controller, this, however, need to be investigated in future work. Overall, the optimization not only improves performance metrics but also offers practical advantages in terms of operational efficiency and system resilience.

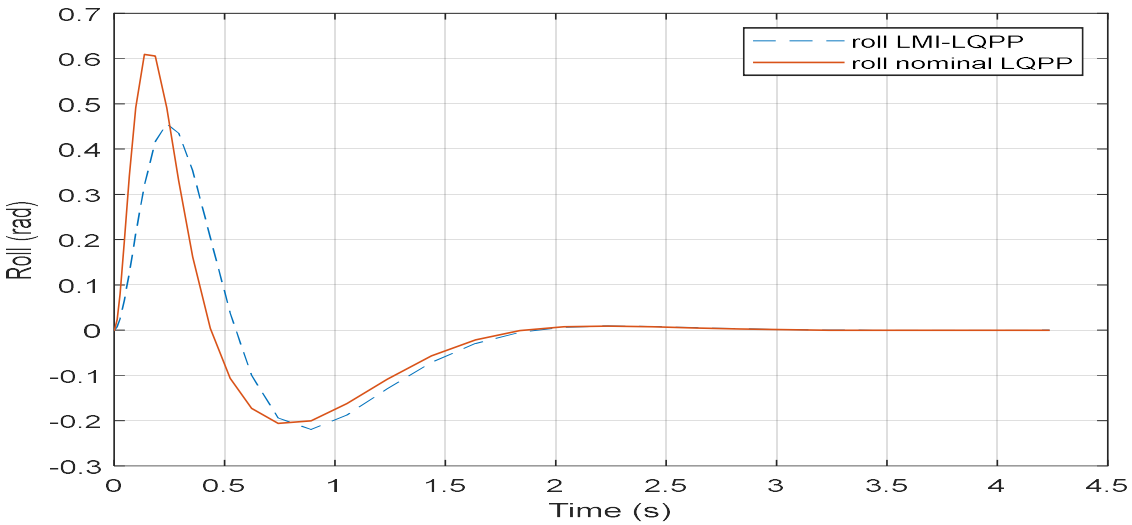

Figure 7 Roll Response to Unit Step Input of LMI-LQPP and Nominal LQPP

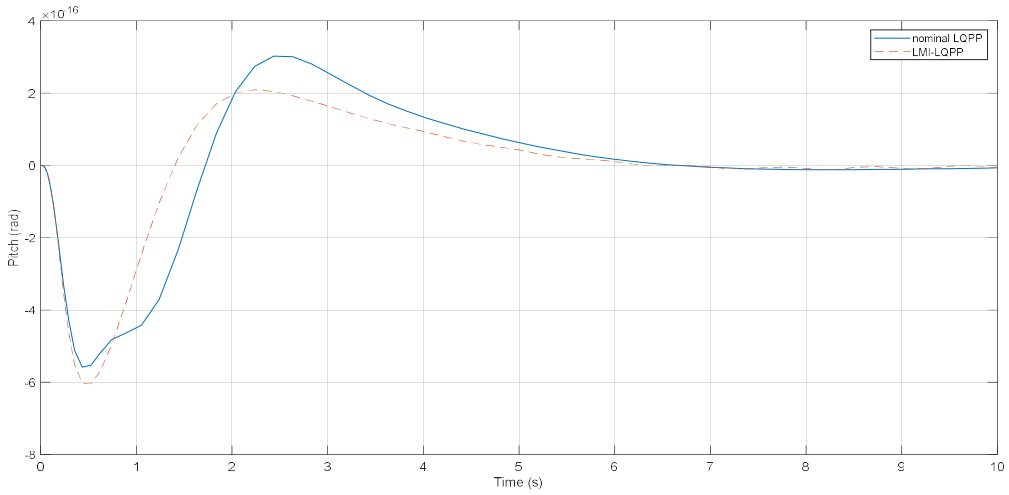

Figure 8 Unit Step Response of Pitch Attitude for LMI-LQPP and Nominal LQPP

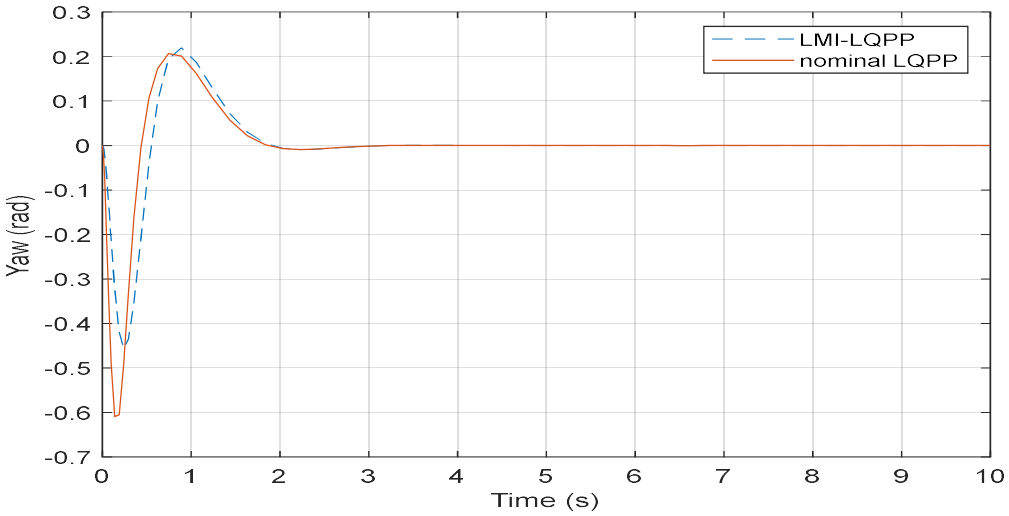

Figure 9: Step Response of Yaw Attitude for Nominal LQPP and LMI-LQPP

Table 3 Performance of attitude response to nominal LQPP and LMI-LQPP

Attitude		Rise time (s)	Settling time (s)	Overshoot (%)	Undershoot (%)	Peak	Peak time (s)
Roll	Nominal LQPP	2.04×10^{-04}	2.2267	60.91	20.63	0.6091	0.1373
	LMI-LQPP	1.29×10^{-04}	2.2824	9.40	21.94	0.4559	0.2385
Pitch	Nominal LQPP	0.0245	6.4727	32.04	56.22	5.58×10^{-16}	0.1373
	LMI-LQPP	0.0247	6.1128	20.52	60.85	4.63×10^{-16}	0.2385
Yaw	Nominal LQPP	0.4521	2.9825	22.02	61.06	0.2202	0.1373
	LMI-LQPP	0.5620	2.9828	20.18	43.94	0.2018	0.2385

IV. CONCLUSION

In conclusion, the application of the LMI-optimized linear quadratic pole-placement (LQPP) state-feedback controller to the quadcopter platform yielded marked enhancements in both attitude and position dynamics compared to the nominal LQPP design. By tuning the feedback gain through convex LMI constraints that penalize control energy under strict stability requirements, a reduction in actuation effort and faster settling time in attitude responses were achieved compared to the nominal design approach. Performance analyses verified that key transient characteristics improved due to the convex nature of the LMI optimization technique. Future work will transition the LMI-based optimized LQPP into a hardware-in-the-loop testbed, integrate it with onboard sensor and actuator drivers, and extend the framework to incorporate fault-tolerant models for actuators and sensors as well as adaptive LMI formulations to accommodate varying payloads and unsteady aerodynamic disturbances.

AUTHOR CONTRIBUTIONS

A. G. Ibrahim: Conceptualization, Methodology, Validation, Writing – original draft, **J. D. Jiya:** Writing – review & editing, Software, Data curation, Visualization, Writing – review & editing. **E. C. Anene:** Proof-reading, Validation, Writing – review & editing.

ACKNOWLEDGEMENT(S)

The researchers wish to extend their sincere gratitude Abubakar Tafawa Balewa University, Bauchi for providing licensed MATLAB software, the Department of Electrical and Electronics Engineering, Abubakar Tafawa Balewa University, Bauchi, Nigeria for the approving the use of its control research facilities, and also to Petroleum Technology Development Fund (PTDF) for providing funding support for the research.

REFERENCES

Ahmad, F., Kumar, P., Bhandari, A., & Patil, P. (2020) Simulation of the Quadcopter Dynamics with LQR based Control, *Materials Today: Proceedings*, 24, pp. 326–332. Available at: https://doi.org/10.1016/j.matpr.2020.04.282.

Ahmadi Dastgerdi, K., Asadi, D., & Nabavi Chashmi, S. Y. (2022) Fault tolerant control of a quadrotor based on

incremental nonlinear dynamic inversion. *International Journal of Aeronautics and Astronautics*, *3*(1), 28–47. https://doi.org/10.55212/ijaa.1033224

Amiruddin, B. P., Iskandar, E., Fatoni, A., & Santoso, A. (2021) *Deep Learning based System Identification of Quadcopter Unmanned Aerial Vehicle*.2020 3rd International Conference on Information and Communication Technology, Yogyakarta, Indonesia. 24th – 25th November, 2020. DOI: 10.1109/ICOIACT50329.2020.9332059

Andersson, O., Wzorek, M., & Doherty, P. (2017) Deep Learning Quadcopter Control via Risk-Aware Active Learning, *Proceedings of the 31th Conference on Artificial Intelligence (AAAI 2017)*, pp. 3812–3818. Available at: http://aaai.org/ocs/index.php/AAAI/AAAI17/paper/view/14622/14104.

Aslam, M. S., & Bilal, H. (2024) Modeling a Takagi-Sugeno (T-S) fuzzy for unmanned aircraft vehicle using fuzzy controller. *Ain Shams Engineering Journal*, Vol. 15 (10) pg. 1-14. https://doi.org/10.1016/j.asej.2024.102984

Babawuro, A.Y., Tahir, N. M., Muhammed, M., & Sambo, A. U. (2020) Optimized state feedback control of quarter car active suspension system based on LMI algorithm', *Journal of Physics: Conference Series*, 15(02). Available at: https://doi.org/10.1088/1742-6596/1502/1/012019

Bose, S., Hote, Y. V., & Hanwate, S. (2019). Analysis of Initial Undershoot in Step Response of Type-1 Nonminimum Phase Systems. *Proceedings of 2019 IEEE Region 10 Symposium, TENSYMP 2019*, 28–32. https://doi.org/10.1109/TENSYMP46218.2019.8971176

Carrio, A., Sampedro, C., & Rodriguez-Ramos, A. (2017) A Review of Deep Learning Methods and Applications for Unmanned Aerial Vehicles, *Journal of Sensors*, 2017, pp. 1–13. Available at: https://doi.org/10.1155/2017/3296874.

Cedro, L., Wieczorkowski, K., & Szcześniak, A. (2024) An Adaptive PID Control System for the Attitude and Altitude Control of a Quadcopter. *Acta Mechanica et Automatica*, *18*(1), 29–39. https://doi.org/10.2478/ama-2024-0004

Datta, S. (2017) Feedback Controller Norm Optimization for Linear Time Invariant Descriptor Systems with Pole Region Constraint, *IEEE Transactions on Automatic Control*, 62(6), pp. 2794–2806.

Deng, X., Sun, X., Liu, R., & Wei, W. (2017) Optimal analysis of the weighted matrices in LQR based on the differential evolution algorithm, *Proceedings of the 29th Chinese Control and Decision Conference, CCDC 2017*, pp. 832–836. Available at: https://doi.org/10.1109/CCDC.2017.7978635

De Oliveira, M. C., & Zheng, Y. (2022). ConvexParameterization of Stabilizing Controllers and its LMI-based Computation via Filtering. *Proceedings of the IEEE Conference on Decision and Control*, 5498–5504. https://doi.org/10.1109/CDC51059.2022.9993254

Duan, G. R., & Yu, H. H. (2013) *LMIs in Control Systems: Analysis, Design and Applications*. Taylor & Francis Group, CRC Press.

Fatkhullin, I., & Polyak, B. (2020) Optimizing static linear feedback: gradient method, SIAM Journal on Control and Optimization. Vol. 59 (5) pp. 1–21. **10.1137/20M1329858**

Gonzalez-Villagomez, J., Rodriguez-Donate, C., Lopez-Ramirez, M., Mata-Chavez, R. I., & Palillero-Sandoval, O. (2023). Novel Iterative Feedback Tuning Method Based on Overshoot and Settling Time with Fuzzy Logic. *Processes*, *11*(3), 694. https://doi.org/10.3390/pr11030694

Howard, D., & Merz, T. (2015) A platform for the direct hardware evolution of quadcopter controllers, *IEEE International Conference on Intelligent Robots and Systems*, 2015-Decem, pp. 4614–4619. Available at: https://doi.org/10.1109/IROS.2015.7354034.

Ka, C. (2002) SIMULTANEOUS LINEAR QUADRATIC POLE PLACEMENT (LQPP) CONTROL DESIGN, in *15th Triennial World Congress, Barcelona, Spain*.

Karam, K., Mansour, A., Khaldi, M., Clement, B., & Ammad-Uddin, M. (2024). Quadcopters in Smart Agriculture : Applications and Modelling. *Applied Sciences*, *14*(19), p.g. 1–26.

Li, T. H. S., & Shieh, M. Y. (2000). Design of a GA-based fuzzy PID controller for non-minimum phase systems. *Fuzzy Sets and Systems*, *111*(2), 183–197. https://doi.org/10.1016/S0165-0114(97)00404-1

Lin, C., Hu, B., Shao, C., Li, W., Li, C., & Xie, K. (2022). Delay-Dependent Optimal Load Frequency Control for Sampling Systems with Demand Response. *IEEE Transactions on Power Systems*, *37*(6), 4310–4324. https://doi.org/10.1109/TPWRS.2022.3154429

Mardijah, D. P. (2022) Control Design of Quadcopter using Output Feedback Control Pole Placement. *Proceeding of the International Conference on Computer Engineering, Network and Intelligent Multimedia, CENIM 2022*. pp. 197-202. ISSN: 9781665476508. doi: 10.1109/CENIM56801.2022.10037547

Martins, L., Cardeira, C., & Oliveira, P. (2019) Linear quadratic regulator for trajectory tracking of a quadrotor, *IFAC-PapersOnLine*, 52(12), pp. 176–181. Available at: https://doi.org/10.1016/j.ifacol.2019.11.195.

Morbale, J., Vidyapeeth, B., Rohan, P., & Vidyapeeth, N. B. (2022) *Quadcopter Drone with Face Recognition*. *August*. https://www.researchgate.net/publication/362517060

Nguyen, N.P., & Hong, S.K. (2018) Sliding mode Thau observer for actuator fault diagnosis of quadcopter UAVs', *Applied Sciences (Switzerland)*, 8(10). Available at: https://doi.org/10.3390/app8101893.

Nguyen, N.P., & Hong, S.K. (2019) Fault-Tolerant control of quadcopter uavs using robust adaptive sliding mode approach, *Energies*, 12(1). Available at: https://doi.org/10.3390/en12010095.

Okyere, E., Bousbaine, A., Poyi, G. T., Joseph, A. K., & Andrade, J. M. (2019) LQR controller design for quad-rotor helicopters, in *9th International Conference on Power*

Electronics, Machines and Drives (PEMD 2018), pp. 4003–4007. Available at: https://doi.org/10.1049/joe.2018.8126.

Pounds, P., Mahony, R., & Corke, P. (2010) Modelling and control of a large quadrotor robot, *Control Engineering Practice*, 18(7), pp. 691–699. Available at: https://doi.org/10.1016/j.conengprac.2010.02.008.

Reizenstein, A. (2017) Position and Trajectory Control of a Quadcopter Using PID and LQ Controllers. [Unpublished] M.Sc Thesis, Division of Automatic Control, Department of Electrical Engineering, Linkoping University, Sweden

Rezende, J. C., Carvalho, L., Neto, J. R. L., Costa, M. V. S., Fortes, E. V., & Macedo, L. H. (2021). LQR design using LMIs and the robust D-stability criterion for low-frequency oscillation damping in power systems. *2021 14th IEEE International Conference on Industry Applications, INDUSCON 2021 - Proceedings*, 188–195. https://doi.org/10.1109/INDUSCON51756.2021.9529623

Sahrir, N. H., & Mohd Basri, M. A. (2022). Modelling and Manual Tuning PID Control of Quadcopter. *Lecture Notes in Electrical Engineering*, *921 LNEE*, 346–357. https://doi.org/10.1007/978-981-19-3923-5_30

Tengis, T., & Batmunkh, A. (2017) Quadcopter stabilization using state feedback controller by pole placement method, *International Journal of Internet, Broadcasting and Communication*, 9(1), pp. 1–8.

Thu, K.M., & Gavrilov, A.I. (2017) Designing and Modeling of Quadcopter Control System Using L1 Adaptive Control, *Procedia Computer Science*, 103(October 2016), pp. 528–535. Available at: https://doi.org/10.1016/j.procs.2017.01.046

Wilt, E., & Sands, T. (2022). Microsatellite Uncertainty Control Using Deterministic Artificial Intelligence. *Sensors*, *22*(22), 8723. https://doi.org/10.3390/s22228723

Xu, D., Whidborne, J.F., & Cooke, A. (2016) Fault tolerant control of a quadrotor using L1 adaptive control, *International Journal of Intelligent Unmanned Systems*, 4(1), pp. 43–66. Available at: https://doi.org/10.1108/IJIUS-08-2015-0011.

Yoon, J., & Doh, J. (2022). Optimal PID control for hovering stabilization of quadcopter using long short term memory. *Advanced Engineering Informatics*, Vol. *53(1) pg. 1-14.* https://doi.org/10.1016/j.aei.2022.101679